

## RESEARCH PAPER

# Mechanisms by which the thiazolidinedione troglitazone protects against sucrose-induced hepatic fat accumulation and hyperinsulinaemia

Fátima O Martins<sup>1,2,3†</sup>, Teresa C Delgado<sup>1,2†</sup>, Joana Viegas<sup>2</sup>, Joana M Gaspar<sup>2</sup>, Donald K Scott<sup>4</sup>, Robert M O'Doherty<sup>4</sup>, M Paula Macedo<sup>2,5‡</sup> and John G Jones<sup>1,5‡</sup>

<sup>1</sup>Metabolic Control Group, Center for Neurosciences and Cell Biology of Coimbra, Cantanhede, Portugal, <sup>2</sup>CEDOC, Chronic Diseases Research Center, NOVA Medical School/Faculdade de Ciências Médicas, Universidade Nova de Lisboa, Lisboa, Portugal, <sup>3</sup>Institute for Interdisciplinary Research (IIIUC), University of Coimbra, Coimbra, Portugal, <sup>4</sup>Division of Endocrinology and Metabolism, University of Pittsburgh, Pittsburgh, PA, USA, and <sup>5</sup>APDP-Diabetes Portugal-Education and Research Center (APDP-ERC), Lisboa, Portugal

### Correspondence

John G. Jones PhD and M. Paula Macedo, Metabolic Control Group, Center for Neurosciences and Cell Biology of Coimbra, UC-Biotech, Biocant Park, Nucleo 4, Lote 8, Cantanhede 3060-197, Portugal.  
E-mail: john.griffith.jones@gmail.com; jones@cnc.uc.pt; paula.macedo@nms.unl.pt  
†These authors contributed equally to this work.  
‡These senior authors also contributed equally to this work.

### Received

20 February 2015

### Revised

13 August 2015

### Accepted

29 September 2015

## BACKGROUND AND PURPOSE

Thiazolidinediones (TZD) are known to ameliorate fatty liver in type 2 diabetes. To date, the underlying mechanisms of their hepatic actions remain unclear.

## EXPERIMENTAL APPROACH

Hepatic triglyceride content and export rates were assessed in 2 week high-sucrose-fed Wistar rats treated with troglitazone and compared with untreated high-sucrose rodent controls. Fractional *de novo* lipogenesis (DNL) contributions to hepatic triglyceride were quantified by analysis of triglyceride enrichment from deuterated water. Hepatic insulin clearance and NO status during a meal tolerance test were also evaluated.

## KEY RESULTS

TZD significantly reduced hepatic triglyceride ( $P < 0.01$ ) by 48%, decreased DNL contribution to hepatic triglyceride ( $P < 0.01$ ) and increased postprandial non-esterified fatty acids clearance rates ( $P < 0.01$ ) in comparison with the high-sucrose rodent control group. During a meal tolerance test, plasma insulin AUC was significantly lower ( $P < 0.01$ ), while blood glucose and plasma C-peptide levels were not different. Insulin clearance was increased ( $P < 0.001$ ) by 24% and was associated with a 22% augmentation of hepatic insulin-degrading enzyme activity ( $P < 0.05$ ). Finally, hepatic NO was decreased by 24% ( $P < 0.05$ ).

## CONCLUSIONS

Overall, TZD show direct actions on liver by reducing hepatic DNL and increasing hepatic insulin clearance. The alterations in hepatic insulin clearance were associated with changes in insulin-degrading enzyme activity, with possible modulation of NO levels.

## Abbreviations

DNL, *de novo* lipogenesis; HOMA-IR, homeostatic model assessment-insulin resistance; IDE, insulin-degrading enzyme; MTBE, methyl tertiary butyl ether; NEFA, non-esterified fatty acids; PDI, protein disulfide isomerase; T2D, type 2 diabetes; TZD, thiazolidinediones; VLDL, very low-density lipoproteins

## Tables of Links

TARGETS	
<b>Nuclear hormone receptors<sup>a</sup></b>	<b>Enzymes<sup>c</sup></b>
PPAR $\alpha$	IDE
PPAR $\gamma$	NOS
<b>Catalytic receptors<sup>b</sup></b>	
<i>IRS1</i>	
<i>IRS2</i>	

LIGANDS	
C-peptide	Nitric oxide (NO)
GSH	Troglitazone
Insulin	

These Tables list key protein targets and ligands in this article which are hyperlinked to corresponding entries in <http://www.guidetopharmacology.org>, the common portal for data from the IUPHAR/BPS Guide to PHARMACOLOGY (Pawson *et al.*, 2014) and are permanently archived in the Concise Guide to PHARMACOLOGY 2013/14 (<sup>a,b,c</sup>Alexander *et al.*, 2013a,b,c).

## Introduction

Thiazolidinediones (TZD) are widely used for improving glycaemic control in type 2 diabetes (T2D) patients. TZD have been also shown to decrease hepatic triglyceride levels in those patients that present non-alcoholic fatty liver disease – a frequent complication of T2D (Belfort *et al.*, 2006; Ratziu and Poynard, 2006). TZD activate the  $\gamma$  isoform of the peroxisome proliferator-activated receptor gamma (PPAR $\gamma$ ) (Lehmann *et al.*, 1995), a nuclear transcription factor that is highly expressed in adipose tissue but is poorly expressed in other insulin sensitive tissues such as skeletal muscle, liver, pancreas, heart and spleen (Ferre, 2004). Thus, adipose tissue is considered to be the main site of action for TZD, and much of their systemic beneficial effects have hitherto been explained via their effects on adipocyte physiology and metabolism. These include accelerated adipocyte uptake, oxidation and esterification of circulating non-esterified fatty acids (NEFA), thereby reducing the ectopic lipid burden and its interference of insulin signalling in other tissues such as the skeletal muscle and liver. This is accompanied by alterations in adipokine secretion profile that can further improve control of glucose and lipid metabolism in these tissues (Guan *et al.*, 2002; Boden *et al.*, 2005). However, adipose tissue may not be the exclusive site of action for TZD. Lipoatrophic patients have negligible adipose tissue mass, and the same is true for a mouse model of late onset lipoatrophy. Yet in both settings, TZD therapy was shown to improve diabetes and hyperlipidaemia (Burant *et al.*, 1997; Arioglu *et al.*, 2000).

In the liver, TZD have been shown to reduce the expression of gluconeogenic enzymes in animal models (Way *et al.*, 2001) and attenuate gluconeogenic fluxes in T2D patients (Gastaldelli *et al.*, 2006). In addition to being a principal control site for carbohydrate metabolism, the liver is also highly involved in regulating systemic lipid fluxes via re-esterification, lipogenesis and very low-density lipoproteins (VLDL) export. Furthermore, it plays an active role in controlling the levels of circulating insulin via first-pass clearance of secreted insulin mediated by insulin-degrading enzyme (IDE) and protein disulfide isomerase (PDI) (Osei *et al.*, 2007; Lamontagne *et al.*, 2013). Recently, it has been suggested that NO attenuates insulin clearance (Natali *et al.*, 2013) via inhibition of IDE (Cordes *et al.*, 2009). Decreased insulin clearance has been associated with hyperinsulinaemia and decreased insulin sensitivity (Ader *et al.*, 2014; Bril *et al.*, 2014).

Thus, the development of steatosis and hyperinsulinaemia, which in addition to glucose intolerance are defining features of the insulin resistant state, may reflect dysfunctional hepatic lipid metabolism as well as impaired hepatic insulin clearance. We hypothesized that TZD ameliorate steatosis and hyperinsulinaemia through changes in hepatic lipid fluxes and insulin clearance. To test this hypothesis, we chose troglitazone, the first TZD to be used as an antidiabetic drug. Troglitazone was subsequently withdrawn from clinical use due to severe hepatotoxicity, confirmed in subsequent studies with human primary hepatocyte cultures and cell lines (Yamamoto *et al.*, 2002). Troglitazone is better tolerated by rat hepatocytes (Lauer *et al.*, 2009). For both Gunn and Wistar rats, there were no indications of liver injury following long-term administration of troglitazone at 400 mg·kg<sup>-1</sup>·day<sup>-1</sup>. This dosage is well above those previously used to study its antidiabetic effects (Lee *et al.*, 1994; Khoursheed *et al.*, 1995; Okuno *et al.*, 1998) as well as that used in our present study.

We tested the hepatic effects of troglitazone in rodent models of short-term (14 day) high-sucrose feeding. This model is useful for specifically probing splanchnic complications of diet-induced insulin resistance because steatosis and hyperinsulinaemia are established before significant increases in whole-body adiposity. Moreover, troglitazone has been shown to be more effective in reversing insulin resistance and glucose tolerance in models of high sugar and fructose feeding (Lee *et al.*, 1994; Santure *et al.*, 2003) compared with high-fat feeding (Khoursheed *et al.*, 1995). It is well known that high sucrose feeding induces a substantial increase in *de novo* lipogenesis (DNL) such that this pathway becomes a significant contributor to hepatic triglyceride synthesis (Chong *et al.*, 2007; Richelsen, 2013). Therefore, we further hypothesized that the reversal of steatosis in this setting by TZD involves the attenuation of hepatic DNL.

## Methods

### Animals

All animals were handled according to the European Union guidelines for the use of experimental animals (2010/63/EU). The experiments were approved by the Ethics Committee of the Faculty of Medical Sciences at the New University

of Lisbon. All animal care and experimental procedures complied with the ARRIVE guidelines (Kilkenny *et al.*, 2010; McGrath *et al.*, 2010). Thirty-six 12-week-old male Wistar rats were maintained in a 12 h light/12 h dark cycle (lights on from 07 h to 19 h) with *ad libitum* access to food and water. Animals were randomly separated in standard chow (SC), HS-fed rodents (HS-C) (35% w v<sup>-1</sup> in drinking water) and troglitazone-treated HS-fed rodents (0.2%, included in the diet) (HS-T). The troglitazone dose was selected from previous studies like the one from Okuno and colleagues (Okuno *et al.*, 1998). The animals were maintained on these diets for 14 days with water and food consumption being recorded. Caloric intake was calculated taking into account these data, the calories from the diet used in the animal facility and by the following equations:

$$\begin{aligned} \text{Calories from food} &: (\text{average daily weight food(g)}) * 437,1 / 199 \\ \text{Calories from beverage (HS-C and HS-T groups)} &: \\ & (\text{average daily water with sucrose(ml)}) * 35 * 4 / 100 \end{aligned}$$

Two parallel studies were conducted with 18 animals per study, six per diet regime. In study 1, hepatic DNL and VLDL export were measured. At 19 h of day 13, all animals of study 1 received a loading dose of 99% <sup>2</sup>H<sub>2</sub>O (3 g 100 g<sup>-1</sup> body weight), and the drinking water was also supplemented with <sup>2</sup>H<sub>2</sub>O to a 3% final enrichment. Following overnight *ad libitum* feeding, animals were sacrificed the next morning after cervical dislocation following ketamine i.p. injection (100 mg·kg<sup>-1</sup> body weight). The liver and epididymal adipose tissue were then immediately excised, weighed and freeze-clamped in liquid nitrogen until further analysis.

In study 2, food was withdrawn on the last evening (day 13), and animals were fasted overnight. On the morning of day 14, rats were allowed *ad libitum* access to their respective diets for 120 min. At predetermined intervals, plasma NEFA, glucose, insulin and C-peptide levels were quantified. Rate constants for the decrease in plasma NEFA concentrations were derived from the logarithm-transformed curves of the relative reduction in plasma NEFA concentrations from 0 to 120 min (Daly *et al.*, 1998). Livers were excised and immediately freeze-clamped in liquid nitrogen until further analysis for enzyme activities, NO levels and protein expression.

### Quantification of hepatic DNL

Hepatic triglycerides can be derived from plasma NEFA, which are taken up via lipoprotein transport and esterified to triglycerides after hepatic uptake. They can also be formed *in situ* by DNL of fatty acids from acetyl-CoA. Hepatic DNL was quantified using <sup>2</sup>H<sub>2</sub>O as previously reported (Delgado *et al.*, 2009; Soares *et al.*, 2012). From the <sup>1</sup>H and <sup>2</sup>H NMR data, triglyceride methyl <sup>2</sup>H-enrichment levels were estimated, and by relating these enrichments values to that of plasma water, the contribution of DNL to total hepatic triglycerides was calculated.

After the livers had been dried by lyophilization, about half of each liver was powdered and a Folch extraction, with 20 mL chloroform : methanol (2:1) g<sup>-1</sup> dried tissue, performed. The mixture was continuously agitated for 20 min at room temperature and then centrifuged for 5 min at 4°C and 1500 g. The supernatant was vigorously mixed with

100 mL 0.9% (w v<sup>-1</sup>) NaCl and then centrifuged for 5 min at 4°C and 1500 g. The upper phase was discarded, and the lipid-containing lower phase was recovered and evaporated to dryness. Afterwards, dried lipids were dissolved in 2 mL hexane/methyl tertiary butyl ether (MTBE) (200:3) solution for purification by solid-phase extraction.

For triglyceride purification, reverse phase solid-phase extraction columns (Discovery DSC-18, Sigma-Aldrich, Steinheim, Germany) (2 g) were initially washed with 12 mL of hexane/MTBE (96:4) followed by 12 mL hexane. The lipid fraction was added to the column and further washed with 10 mL hexane/MTBE (200:3). To recover triglycerides, 12 mL hexane/MTBE (96:4) was eluted in the column, and 1 mL fractions were collected. For identification of the fractions containing triglycerides, thin layer chromatography was performed using a mixture of petroleum ether, diethyl ether and acetic acid in the proportions of 8.0:2.0:0.1 as elutant and visualization by iodine. Finally, triglyceride fractions were combined and evaporated to dryness for NMR analysis.

For the acquisition of <sup>1</sup>H and <sup>2</sup>H NMR spectra, the purified triglyceride extract was dissolved in 300 µL of chloroform, and deuterated pyrazine was used as an internal <sup>2</sup>H-enrichment standard. <sup>1</sup>H and <sup>2</sup>H NMR spectra were acquired at 25°C with a 14.1 T Varian Spectrometer (Varian, Palo Alto, CA, USA) equipped with a 3 mm broadband probe. Proton-decoupled <sup>2</sup>H NMR spectra were acquired without lock. Acquisition parameters included a free induction decay acquisition time of 5 s, a delay of 2 s and a 90° pulse width. Between 500 and 1000 transients were acquired to achieve adequate signal to noise for signal area analysis. Spectra were referenced for tetramethylsilane using the peaks of chloroform and pyrazine resonances, at 7.27 and 8.60 p.p.m. respectively. Before Fourier transformations, <sup>1</sup>H and <sup>2</sup>H NMR spectra were multiplied by 0.5 and 1.0 Hz Lorentzian functions, respectively, and signal areas determined using the signal deconvolution routine of the PC-based NMR processing software NUTS proTM (Acorn, Fremont, CA, USA). Plasma water <sup>2</sup>H-enrichments were determined from plasma by <sup>2</sup>H NMR spectroscopy analysis, as described previously (Jones *et al.*, 2001). Briefly, a 10 µL volume of plasma was mixed with a known amount of acetone, and the <sup>2</sup>H-enrichments were determined using a standard curve constructed previously using <sup>2</sup>H<sub>2</sub>O-enrichment standards against the constant natural abundance <sup>2</sup>H signal of the acetone.

### Quantification of hepatic VLDL-triglyceride export rates

Hepatic VLDL-triglycerides export rates were determined according to Millar *et al.* (Millar *et al.*, 2005). On the morning of day 14 following overnight *ad libitum* feeding, rats were given an i.p. injection of poloxomer 407 (1000 mg·kg<sup>-1</sup> body weight). Plasma triglycerides were evaluated immediately before and at pre-established time intervals after poloxomer 407 injection. Hepatic VLDL-triglycerides export rates were derived from the slope of the curves of plasma triglycerides concentrations at 0–90 min.

### Biochemical assays

Plasma glucose was assessed using a standard glucometer, whereas the quantitative determination of plasma insulin and C-peptide levels was achieved by means of ELISA

(Mercodia AB, Uppsala, Sweden). Plasma NEFA levels were assessed using an *in vitro* enzymatic colorimetric method assay (Wako Chemicals GmbH, Neuss, Germany). Plasma triglycerides and hepatic and epididymal adipose tissue triglycerides were determined, following a Folch extraction of the tissue samples, by an automated clinical chemistry analyser (Olympus AU400 Chemistry Analyzer, Beckman Coulter Inc., CA, USA).

### Assessment of insulin clearance, HOMA-IR and HOMA- $\beta$

After quantification of plasma insulin and C-peptide levels, insulin clearance was calculated by the ratio between C-peptide, a surrogate of insulin secretion, and plasma insulin levels for each point analysed. Homeostatic model assessment (HOMA) indices were assessed from basal (fasting) glucose and insulin [homeostatic model assessment-insulin resistance (HOMA-IR)] or fasting glucose and C-peptide concentrations (HOMA- $\beta$ ) according to the recommendations of Wallace *et al.* (Wallace *et al.*, 2004). HOMA- $\beta$  gives an indication of  $\beta$ -cell secretion, while HOMA-IR gives an indication of insulin resistance under basal fasting conditions.

### Assessment of hepatic NO levels

Liver was degraded by mechanical disruption using a piston in a buffer containing Tris-HCl 25 mM (pH 7.4), EDTA 1 mM and EGTA 1 mM. Extracts were centrifuged and supernatant denatured with ethanol. Hepatic NO levels were measured by a chemiluminescent-based technique using a Sievers 280 NO Analyzer (Sievers Instruments, Boulder, CO, USA) as previously described (Afonso *et al.*, 2006).

### Evaluation of hepatic NOS, IDE and PDI activities

For nitric oxide synthase (NOS) activity, a buffer composed of 25 mM Tris-HCl, pH 7.4, 1 mM EDTA and 1 mM EGTA was used to degrade the tissue in combination with mechanical homogenization. The resulting extracts were centrifuged, and supernatants were measured for NOS activity using the Ultra-sensitive Assay for NOS kit (Oxford Biomedical Research, Oxford, MI, USA). For quantification of IDE activity, liver tissue was also degraded by mechanical homogenization in a buffer containing 170 mM NaCl and 2 mM EDTA. The FRET substrate Mca-GGFLRKHGQ-EDDnp was added to the homogenate, and a fluorometric assay was performed as previously described (Miners *et al.*, 2008). PDI activity was measured after incubation of homogenized liver tissue for 1 h at 37° with Krebs-Henseleit rinsing buffer supplemented with CaCl<sub>2</sub> and collagenase (50 mg). Samples were then centrifuged at 4° and 16000 g for 5 min two times, with recovery of the pellet containing the hepatocytes between centrifugations and resuspension in Krebs-Henseleit rinsing buffer. The final pellet was resuspended in lysis buffer containing 50 mM Tris-HCl, 300 mM NaCl, 1:200 dilution of tablet protease cocktail inhibitor and 1% Triton X-100. The mixture was submitted to five bursts of low-level sonication and then centrifuged at 16000 g for 30 min at 4°. The supernatant was kept, and PDI activity was measured at 630 nm by an OD assay over a 60 min period. The reaction mixture was composed of distilled water, 10 mM potassium phosphate buffer (pH 7.4), 8 mM GSH and 1.16 mg·mL<sup>-1</sup> insulin

with a final volume of 186  $\mu$ L. To this, 10  $\mu$ L of the supernatant was added to each well in a multi-well plate. In this assay, the PDI promotes the cleavage of insulin present in the reaction mixture, and the insulin degradation products cause an increase in OD that is proportional to the units of PDI present.

### Assessment of protein expression

Protein extracts for Western blot analysis were obtained using a lysis buffer (1 M Tris-HCl, pH 7.5, 0.2 M EGTA, 0.2 M EDTA, 1% Triton-X 100, 0.1 M sodium orthovanadate, 2 g·L<sup>-1</sup> sodium fluoride, 2.2 g·L<sup>-1</sup> sodium pyrophosphate and 0.27 M sucrose) to homogenize liver tissue. Samples were centrifuged, and total protein lysates were kept at -20°. Total protein lysates from liver were subjected to SDS-PAGE, electrotransferred on a PVDF membrane and probed with the respective antibodies: IDE (sc-27265) and PDI (sc-20132) (Santa Cruz Biotechnology, Santa Cruz, CA, USA). Then, membranes were revealed in a ChemiDoc apparatus (Bio-Rad Laboratories, Inc., Hercules, CA, USA). Protein levels were normalized to  $\beta$ -actin (A5316, Sigma) for each sample.

### Data analysis and statistical procedures

Data are expressed as mean  $\pm$  SEM of at least five animals per group. Statistical significance was calculated using one-way ANOVA (Bonferroni *post hoc* test).

### Materials

Troglitazone was procured from Sangyo, Japan. <sup>2</sup>H<sub>2</sub>O (99% enriched) was acquired from CortecNet (Voisins-Le-Bretonneux, France), sucrose for drinking water preparation from Panreac (Castellar del Vallès, Barcelona, Spain) and other reagents from Sigma Aldrich (Steinheim, Germany).

## Results

### Baseline glycaemic and lipidaemic parameters for the group fed with SC and the group fed with high sucrose (HS-C)

Plasma NEFA and triglycerides following an overnight fast or after normal overnight feeding were similar for SC and HS-T (Table 1). Weight gain over the 2 week feeding period was not different between SC and HS-C, although daily caloric intake was significantly increased for HS-C. Total epididymal adipose tissue triglyceride content was not different between SC and HS-C (Table 1). However, in agreement with earlier studies (Huang *et al.*, 2010), hepatic triglyceride levels were threefold higher in HS-C compared with SC (Figure 1). Moreover, fractional DNL rates (Figure 1) were increased approximately twofold in HS-C-fed compared with SC-fed rats. Expression of SREBP1c, a transcription factor promoting the expression of lipogenic enzymes and activated by insulin was also significantly elevated in HS-C-fed compared with SC-fed rats (Figure 1). As shown in Figure 2, postprandial export of hepatic triglyceride via VLDL showed a tendency to be increased in HS-C compared with SC ( $P = 0.16$ ). Also, the clearance of fasting plasma NEFA levels following a

**Table 1**

Weight increase, adiposity and plasma metabolite and hormone levels for rats fed on the three dietary regimes

	Standard chow	High sucrose	High sucrose + troglitazone
Initial weight (g)	293 ± 18	300 ± 16	285 ± 8
2-week weight increase (%)	29 ± 3	23 ± 3	23 ± 2
Chow intake (g day <sup>-1</sup> )	28 ± 1	22 ± 2**	20 ± 1
Troglitazone intake (mg Kg <sup>-1</sup> day <sup>-1</sup> )	176 ± 6	136 ± 13**	133 ± 9**
Caloric intake (kcal day <sup>-1</sup> )	129 ± 5	174 ± 15*	156 ± 8
Plasma NEFA (mmol l <sup>-1</sup> ) <sup>a</sup>	1.66 ± 0.25	1.81 ± 0.21	0.25 ± 0.04**, ##
Plasma NEFA (mmol l <sup>-1</sup> ) <sup>b</sup>	2.19 ± 0.32	1.73 ± 0.42	2.02 ± 0.39
Plasma triglycerides (mmol l <sup>-1</sup> ) <sup>a</sup>	1.11 ± 0.06	1.28 ± 0.18	1.13 ± 0.20
Plasma c-peptide (nmol l <sup>-1</sup> ) <sup>b</sup>	0.45 ± 0.18	0.74 ± 0.30	0.48 ± 0.21
Plasma insulin (µg l <sup>-1</sup> ) <sup>b</sup>	0.4 ± 0.1 <sup>#</sup>	0.9 ± 0.1*	0.2 ± 0.1 <sup>##</sup>
Plasma glucose (mmol l <sup>-1</sup> ) <sup>a</sup>	6.6 ± 0.3	6.3 ± 0.3	6.9 ± 0.3
Plasma glucose (mmol l <sup>-1</sup> ) <sup>b</sup>	4.4 ± 0.2	4.6 ± 0.2	4.7 ± 0.2
HOMA-IR	1.84 ± 0.62 <sup>#</sup>	4.40 ± 0.71*	1.10 ± 0.22 <sup>##</sup>
HOMA-β	15.5 ± 8.7	21.0 ± 8.9	8.4 ± 10.3
Epididymal fat pads weight (g)	5.1 ± 0.5	6.1 ± 0.7	6.6 ± 0.8
Total epididymal adipose tissue triglycerides (mg g <sup>-1</sup> body wt) <sup>b</sup>	1.0 ± 0.1	1.1 ± 0.1	1.3 ± 0.2

\**P* < 0.05 and\*\**P* < 0.01 relative to the SC group;#*P* < 0.05 and##*P* < 0.01 relative to the HS group.<sup>a</sup>Following overnight *ad libitum* feeding.<sup>b</sup>Following overnight fast.

120 min feeding period was significantly slower for HS-C compared with SC, as shown in Figure 3.

Plasma glucose levels either after overnight fasting or after normal overnight feeding were not significantly different between SC and HS-C groups indicating that glycaemic control was maintained with HS feeding. However, fasting plasma insulin levels were significantly higher for HS-C versus SC. This translates to a significantly higher HOMA-IR index (Table 1) and indicates a compensated insulin-resistant state for HS-C relative to SC. Meal-induced blood glucose, plasma insulin, C-peptide excursions and insulin clearance were not different between HS-C and SC (Figure 4). Hepatic IDE activity was not different between HS-C and SC animals, but PDI activity was significantly decreased in HS-C compared with SC animals (Figure 5). Regarding IDE and PDI expression, there were no alterations between SC-fed and HS-C-fed animals (Figure 5). Finally, there were no alterations in NO levels and NOS activity in HS-C-fed animals at 2 weeks of sucrose feeding (Figure 6).

### Effects of troglitazone administration in rats fed with a high sucrose diet

For animals that were placed on an HS diet and also administered with troglitazone (HS-T), neither weight gain nor caloric intake over the 2 week feeding period was different

compared with HS-C or SC. Epididymal adipose tissue triglyceride content was not different compared with either SC or HS-C. However, hepatic lipid levels were significantly reduced compared with HS-C and were indistinguishable from SC. These reductions in hepatic triglyceride were associated with significant reductions in fractional DNL rates to levels that were similar to SC (Figure 1). With troglitazone, SREBP1c expression showed a tendency for reverting to the lower levels measured in SC (*P* = 0.095 for HS versus HS-T, Figure 1). Differences in rates of hepatic VLDL-triglyceride export were not significant but showed a tendency to be reduced in HS-T compared with HS-C (Figure 2). HS-T had similar fasting plasma NEFA and triglycerides levels to both HS-C and SC (Table 1) suggesting that there was no significant effect of troglitazone supplementation on fasting whole-body triglyceride dynamics. However, under fed conditions, HS-T had significantly lower plasma NEFA levels compared with both HS-C and SC (Table 1). Moreover, troglitazone potentiated the drop in plasma NEFA levels following the transition from fasting to feeding, with the fractional decrease in NEFA concentration exceeding both HS-C and SC groups, as shown in Figure 3.

Plasma glucose levels either after overnight fasting or after normal overnight feeding were not significantly different between HS-T and either HS-C or SC groups. However, HS-T had significantly reduced fasting plasma insulin and HOMA-IR

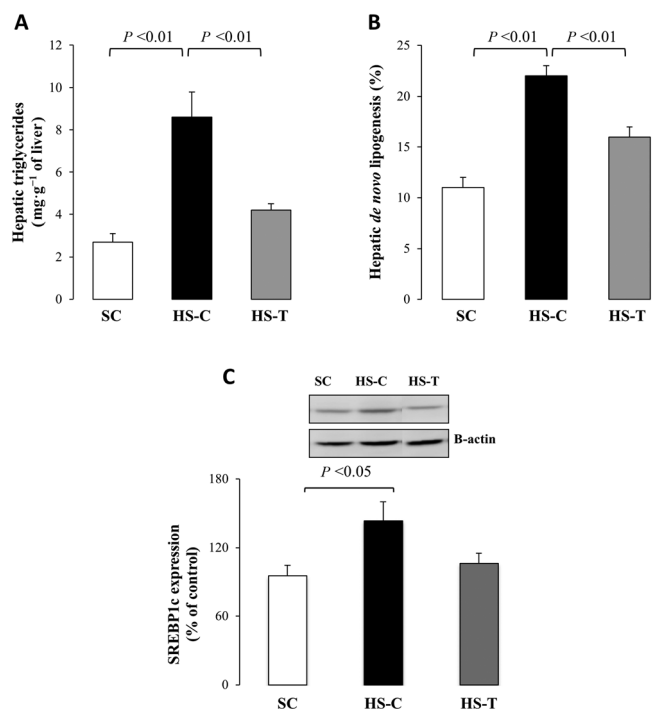


**Figure 1**

Hepatic triglyceride levels (A), fractional contribution of *de novo* lipogenesis to hepatic triglyceride levels (B) and SREBP-1c expression levels relative to  $\beta$ -actin (C), in standard-chow (SC), high-sucrose (HS-C) and in 2 weeks troglitazone-treated high-sucrose-fed (HS-T) rodents.

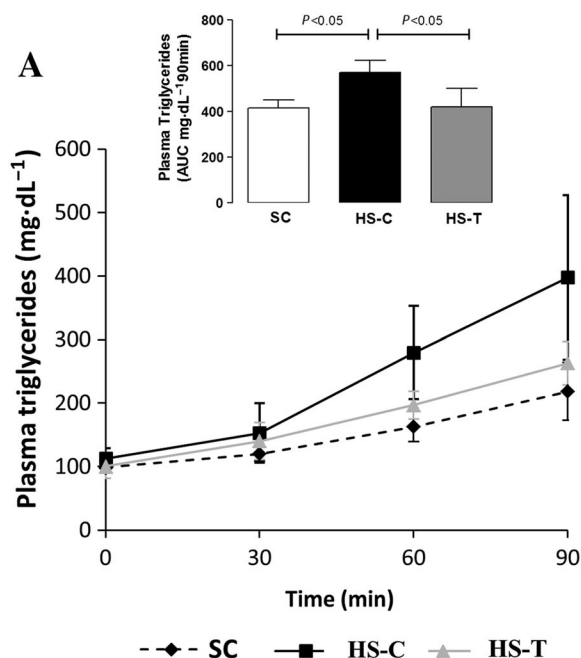


**Figure 2**

Quantification of very low-density lipoproteins (VLDL)-triglycerides export rates following inhibition of adipose tissue lipolysis, by means of poloxamer 407 injection, after overnight *ad libitum* feeding. (A) Graphical representation of the accumulation of plasma triglycerides during 90 min and (B) average of the slopes of the curves of plasma triglycerides concentrations at 0–90 min for standard-chow (SC), high-sucrose (HS-C) and 2 weeks troglitazone-treated high-sucrose-fed (HS-T) rodents.

values compared with HS-C and were similar to SC regarding insulin sensitivity (Table 1). The HS-T group had a pattern of plasma glucose excursion following a meal that was identical to HS-C and SC groups. While meal-induced C-peptide profiles were not significantly different between the three groups, plasma insulin levels were significantly lower in HS-T compared with either HS-C or SC (Figure 4). These data indicate that the reduced insulin levels were due to increased hepatic insulin clearance rather than reduced pancreatic insulin secretion (Figure 4).

The increase in insulin clearance correlates with an increase in hepatic IDE activity for HS-T (Figure 5). Regarding PDI activity, troglitazone effected no alteration in the decrease promoted by sucrose feeding (Figure 5). IDE and PDI expression were not altered in HS-T animals (Figure 5). Levels of NO, an inhibitor of IDE activity, were significantly diminished in HS-T group, and this was associated with a decrease in NOS activity. Therefore, the observed increase in insulin clearance can be linked to decreased hepatic NO levels, which in turn were associated with increased IDE activity (Cordes *et al.*, 2009) (Figure 6).

## Discussion

Thiazolidinediones are widely used pharmacological agents that improve several aspects of insulin resistance including fatty liver and hyperinsulinaemia (Belfort *et al.*, 2006; Ratzin and Poynard, 2006). Because troglitazone was withdrawn from clinical use due to hepatotoxicity, a potential concern is that the observed hepatic metabolic changes could reflect hepatic injury rather than a true pharmacological effect on

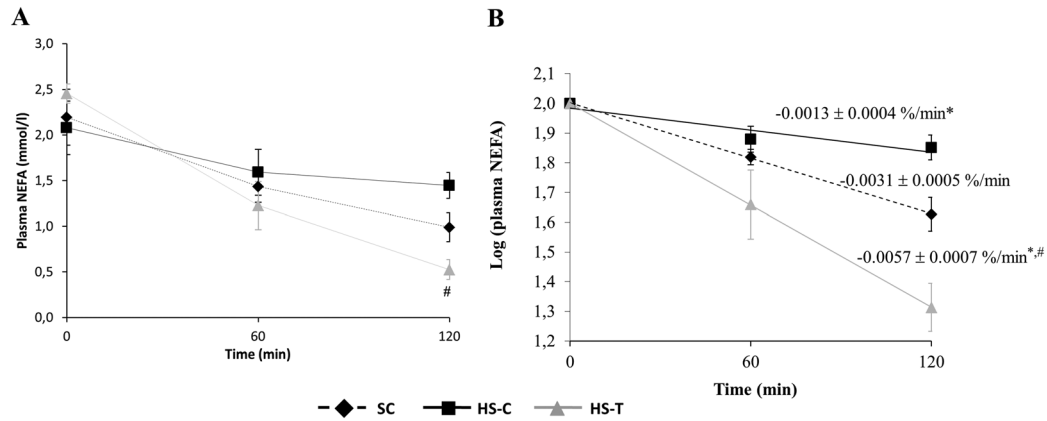


**Figure 3**

(A) Absolute values and (B) logarithm-transformed curves of the relative reduction in plasma NEFA concentrations from 0 to 120 min refeeding, following overnight fast, in standard-chow (SC), high-sucrose (HS-C) and in 2 weeks troglitazone-treated high-sucrose-fed (HS-T) rodents. \* $P < 0.05$  relative to SC and # $P < 0.05$  relative to HS-C are indicated.

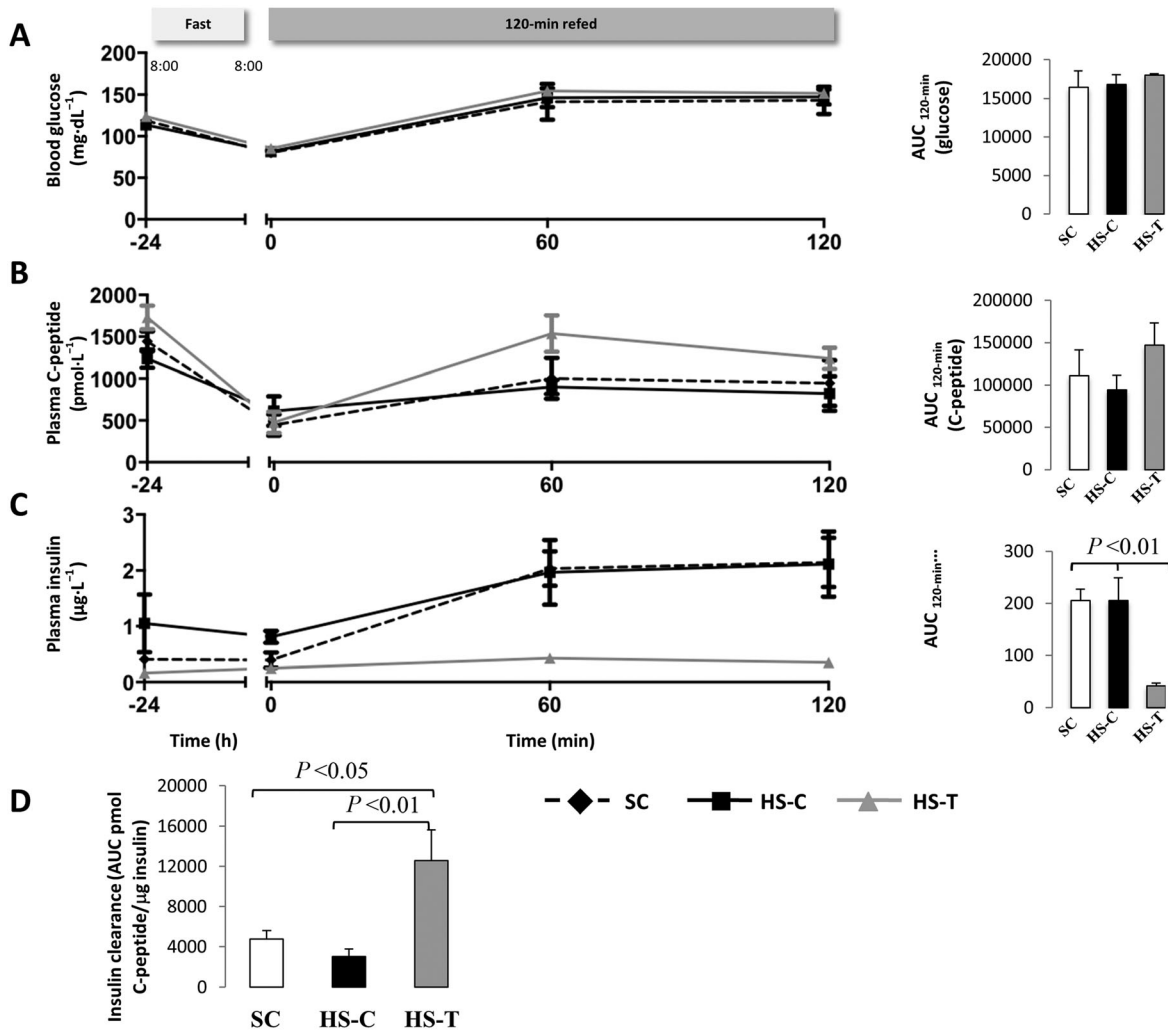


**Figure 4**

Following overnight fast, animals were submitted to 120 min refeeding. (A) Blood glucose; (B) plasma C-peptide; (C) plasma insulin profiles and integration of the AUC; and (D) insulin clearance integration of the AUC during 120 min refeeding in standard-chow (SC), high-sucrose (HS-C) and in 2 weeks troglitazone-treated high-sucrose-fed (HS-T) rodents.

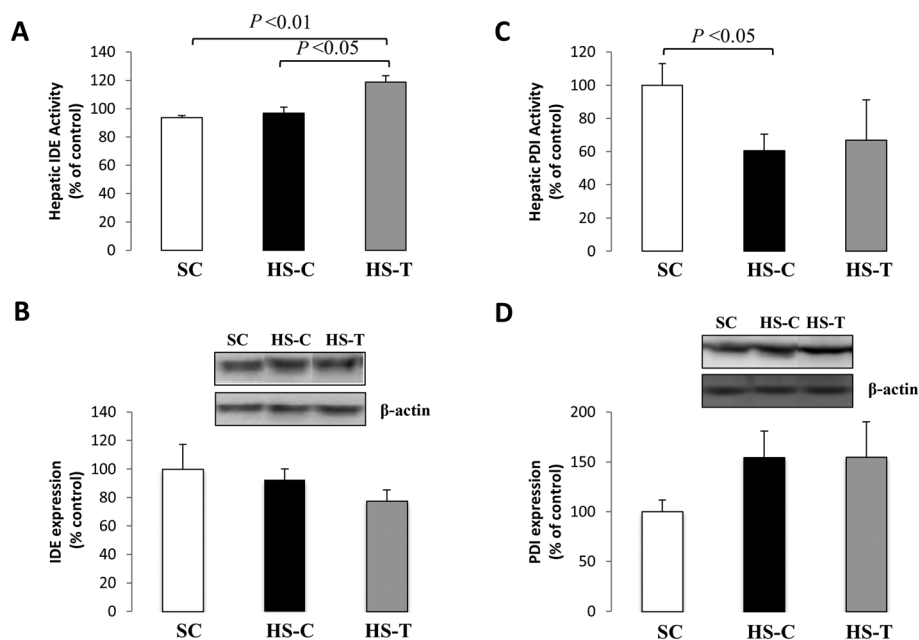


**Figure 5**

Quantification of hepatic enzymes activity and expression. (A) Hepatic insulin-degrading enzyme (IDE) activity; (B) hepatic IDE expression; (C) hepatic protein disulfide isomerase (PDI) activity; and (D) hepatic PDI expression after 120 min refeeding in standard-chow (SC), high-sucrose (HS-C) and in 2 weeks troglitazone-treated high-sucrose-fed (HS-T) rodents.

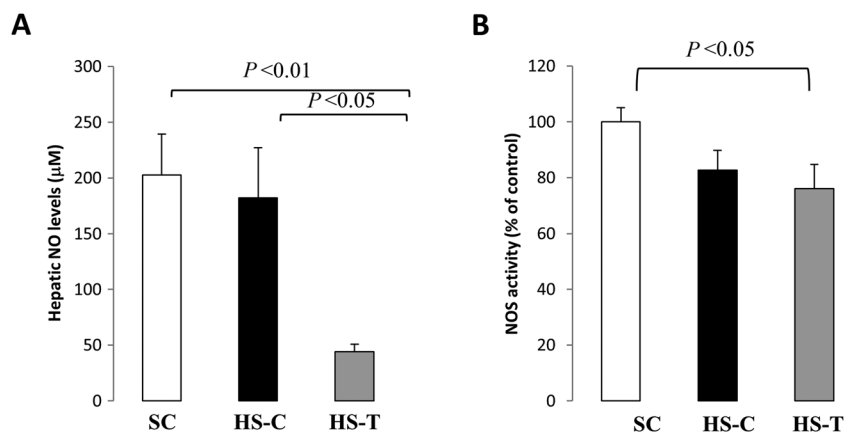


**Figure 6**

Evaluation of hepatic NO production. (A) Hepatic NO levels and (B) hepatic NOS activity after 120 min refeeding in standard-chow (SC), high-sucrose (HS-C) and in 2 weeks troglitazone-treated high-sucrose-fed (HS-T) rodents.

metabolic flux regulation. Amelioration of sucrose or fructose-induced insulin resistance was demonstrated in animals whose feed was supplemented with 0.2g troglitazone per 100g feed (Lee *et al.*, 1994; Santure *et al.*, 2003). In our study, the estimated average daily intake of troglitazone was 133 mg·kg<sup>-1</sup>·day<sup>-1</sup>, well below the level of 400 mg·kg<sup>-1</sup>·day<sup>-1</sup> that was shown not to cause hepatic injury in either Wistar or Gunn rat strains after 3 months of administration (Watanabe *et al.*, 2000).

The purpose of the current study was to better understand the underlying hepatic mechanisms of these actions in the

setting of sucrose-induced hepatic insulin resistance. Our data show that troglitazone prevented the accumulation of hepatic lipids following 2 weeks of HS feeding in rat models. Kawaguchi *et al.* previously showed that pioglitazone protected against steatosis in a 2 week choline-deficient animal model (Kawaguchi *et al.*, 2004). Wei *et al.* reported that another TZD member, pioglitazone, reduced both blood glucose levels and insulin in mice that had been fed a high-fat diet for 6 months (Wei *et al.*, 2014).



Our results demonstrate that troglitazone prevents the accumulation of hepatic lipids in 2 week HS-fed rodents not only by reducing plasma NEFA (presumably by improved adipocyte NEFA uptake) but also by decreasing hepatic DNL. The reduction in DNL appears to be mediated at least in part by a suppression of SREBP1c expression. Given that hepatic SREBP1c expression is known to be stimulated by insulin via Insulin Receptor substrate 1 and 2 phosphorylation (Kohjima *et al.*, 2008), these differences in SREBP1c expression seem inconsistent with the fact that meal-induced stimulation of insulin secretion was similar between the groups, as measured by plasma C-peptide levels (Figure 4). However, troglitazone significantly increased hepatic insulin degradation, which would result in a steeper drop in insulin levels across the hepatic lobule. Given that DNL activity is highest in pericentral and perivenous regions (Schleicher *et al.*, 2015), it is possible that these hepatocytes experienced lower levels of insulin due to the enhancement of hepatic insulin degradation, thereby attenuating hepatic lipogenic activity.

We demonstrated that the increased insulin clearance was associated with elevated hepatic IDE activity, which in turn was correlated with a fall in the levels of two endogenous inhibitors: NO and NEFA.

If the observed decrease in plasma NEFA levels was due to a more efficient uptake and storage in adipocytes, this would be expected to result in an increased adipose tissue mass. While the 2 week troglitazone treatment of our study did not significantly augment either epididymal fat pad weight or adipose tissue triglycerides mass (Table 1), a 4 week rosiglitazone-based therapy in Zucker lean and fatty rats significantly increased the total weight of epididymal fat pads (Sotiropoulos *et al.*, 2006). Therefore, it is possible that for over a longer period of HS feeding with troglitazone administration, epididymal fat mass would have also shown an increase over untreated HS-fed animals. Therefore, with our short-term HS feeding, the observed plasma NEFA decrease can be mainly attributed to changes in hepatic fat metabolism.

The fatty acyl sources of hepatic triglycerides include plasma NEFA released from adipocytes during fasting, dietary fat intake during feeding and hepatic DNL. Although TZD are well known to stimulate DNL in adipocytes, their effects on hepatic lipogenesis are more controversial. Here, we showed that troglitazone therapy was associated with a decrease in fractional DNL for HS-fed rodents. Likewise, pioglitazone reduced steatosis in a diet-induced steatohepatitis animal model through suppression of liver lipogenic gene expression, including sterol regulatory element-binding protein-1c and fatty acid synthase (Ota *et al.*, 2007). On the other hand, prolonged rosiglitazone-based and troglitazone-based therapy in obese KKA<sup>y</sup> mice, expressing elevated hepatic PPAR $\gamma$ , was associated with a worsening of steatosis and activation of lipogenic genes and DNL (Bedoucha *et al.*, 2001). This suggests that administration of TZD when hepatic expression of PPAR $\gamma$  is constitutively high may promote rather than curtail hepatic steatosis.

Recently, Recently, Beysen *et al.* demonstrated that rosiglitazone and pioglitazone had different effects on hepatic DNL rates in T2D subjects (Beysen *et al.*, 2008). A possible explanation is that the actions of a given TZD may be further potentiated by cross-reactivity with PPAR $\alpha$ , whose agonists are known to increase hepatic fatty acid oxidation activity and reduce

hepatic lipogenic fluxes (Tenenbaum and Fisman, 2012). Moreover, in addition to functioning as PPAR agonists, TZD may also differentially modify PPAR $\alpha$  and PPAR $\gamma$  expression. Thus, troglitazone, an agonist for both PPAR $\alpha$  and PPAR $\gamma$ , was also found to increase PPAR $\alpha$  expression while reducing PPAR $\gamma$  expression in mononuclear cells of obese subjects (Aljada *et al.*, 2001). In the liver, where constitutive PPAR $\alpha$  levels are much higher than those of PPAR $\gamma$ , the anti-lipogenic effects of troglitazone are best explained through its promotion and stimulation of PPAR $\alpha$ .

Thiazolidinedione therapy is also associated with a reduction in peripheral serum insulin levels that accompanies an improvement in insulin sensitivity (Osei *et al.*, 2004; Kim *et al.*, 2005). The insulin-sensitizing effects of PPAR $\gamma$  agonists, such as TZD, were recently attributed to an inhibition of an insulin-signalling cascade, the MEK/ERK pathway, by specifically blocking PPAR $\gamma$  phosphorylation at S273. This cascade has also been linked with increased insulin resistance, which led the authors to open a window for resurrecting PPAR $\gamma$ -targeted therapeutics to improved insulin sensitivity (Banks *et al.*, 2015). In this study, the authors also showed an improvement in glucose tolerance and a decrease in plasma insulin levels in animals treated with MEK inhibitors. However, the mechanism that accounts for the reduced circulating insulin levels remains uncertain.

After insulin is secreted into the portal vein, a significant and variable fraction (40–70%) is immediately cleared by the liver, this fraction being sensitive to physiological and nutritional parameters that also inform insulin sensitivity (Radziuk and Morishima, 1985). Hence, plasma insulin levels reflect both  $\beta$ -cell secretion and hepatic insulin clearance. Insulin clearance is initiated by the binding of insulin to its hepatic receptor. Internalization of the bound insulin complex is critical not only for insulin clearance but also for hepatic insulin actions. It has been suggested that 80% of secreted insulin binds to liver receptors. After binding, insulin can be either fully degraded or returned to the circulation either intact or partially degraded. Insulin clearance is primarily mediated by IDE and PDI (Duckworth *et al.*, 1998). In troglitazone-treated HS-fed rodents,  $\beta$ -cell insulin secretion, quantified using plasma C-peptide as a surrogate (Polonsky and Rubenstein, 1984; Polonsky *et al.*, 1984a), was not altered. Hence, the observed decrease in plasma insulin levels in troglitazone-treated rodents is explained by increased hepatic insulin clearance, given by the ratio between C-peptide levels and plasma insulin levels. In agreement with our study, rosiglitazone therapy increased hepatic insulin clearance in nondiabetic insulin-resistant, impaired glucose tolerant and T2D subjects (Kim *et al.*, 2005; Osei *et al.*, 2007). The observed increase of hepatic insulin clearance is supported, at least in part, by the observed IDE activity increase. Previously, it has been shown that increased insulin sensitivity in both animals and human studies was associated with a stimulation of insulin clearance and decreased hyperinsulinaemia (Ahren and Thorsson, 2003; Ader *et al.*, 2014). However, Maianti *et al.* demonstrated that IDE inhibitors improved glucose tolerance over the short term (Maianti *et al.*, 2014).

Both glucose and NEFA are potential regulators of IDE activity (Hamel, 2009; Pivovarova *et al.*, 2009). Because postprandial glucose excursions were very similar between the three groups, the differential effects of glucose on insulin

clearance between the groups were likely to be insignificant. Studies on the effects of NEFA on IDE-mediated insulin clearance have yielded some contradictory conclusions. On the one hand, the studies of Wei *et al.* indicate that NEFA, specifically palmitate, induces IDE protein and activity (Wei *et al.*, 2014). Meanwhile, other studies indicate that NEFA inhibit insulin degradation via IDE (Hamel, 2009). *In vivo*, the net outcome of these opposing effects of NEFA on insulin clearance ultimately rests on the relative potency of NEFA in inducing IDE protein versus their inhibition of IDE activity. An acute twofold increase of NEFA in lean subjects promoted a pronounced reduction in insulin clearance independently of glucose levels (Hennes *et al.*, 1997; Xiao *et al.*, 2006). This suggests that at least under these short-term conditions, the dominant effect of NEFA was the inhibition of IDE activity, with no major alterations on IDE expression. With long-term high-fat feeding, it is possible that there is a compensatory induction of IDE to counter the effects of chronically excessive NEFA levels, thereby explaining the observations of Wei *et al.* (Wei *et al.*, 2014). Most significantly however, the study of Wei *et al.* and our work taken together indicate that promotion of IDE activity and improvement of hyperinsulinaemia by TZD is a robust outcome regardless of whether insulin resistance was established via long-term high-fat diet or by shorter-term HS feeding.

NO has also been shown to be a regulator of IDE activity. Cordes and colleagues showed that NO directly binds to IDE leading to its inhibition (Cordes *et al.*, 2009). We showed that TZD treatment resulted in a significant decrease of hepatic NO levels and NOS activity. Previous studies demonstrated that pioglitazone administration led to a decrease in inducible NOS (iNOS) activation in obese T2D subjects (Esterson *et al.*, 2013). These specific effects were only observed in T2D patients, where iNOS activity is elevated compared with healthy subjects.

While IDE is considered to be the primary enzyme for hepatic insulin clearance, PDI, which is also expressed by the liver, can also alter internalized insulin. The disulfide bonds between the two chains of insulin can be cleaved by PDI action, allowing some reactions between the separated chains and reactive molecules surrounding them. Namely, it is known that these chains can undergo nitrosylation by PDI-derived activity (Zai *et al.*, 1999; Root *et al.*, 2004). Moreover, it is known that PDI activity increase has been associated to states of higher insulin sensitivity, namely, in the postprandial state (Mikami *et al.*, 1998). Therefore, our data indicate that hepatic PDI activity and expression were not correlated with either IDE activity or insulin clearance, but it is possible that PDI may have a role in insulin degradation that is downstream or complementary to that of IDE in specific conditions.

In conclusion, our data demonstrate that troglitazone protects against hepatic fat accumulation induced by a short-term period of high sucrose feeding via several mechanisms, acting in concert, involving both adipose tissue and liver. In addition to the canonical mechanism of increased adipocyte NEFA uptake and esterification, thereby reducing plasma NEFA, we also demonstrated an inhibition of hepatic DNL and also reduced hepatic NO levels and NOS expression. The reduction in hepatic lipid and NO, both of which are inhibitors of IDE, was correlated with an increase in IDE activity and hepatic insulin clearance. This increased insulin

clearance explained the maintenance of normal plasma insulin levels concomitant with the preservation of insulin sensitivity. These novel hepatic actions of TZD offer more precise therapeutic strategies for reversing the onset of non-alcoholic fatty liver disease and countering hyperinsulinaemia in T2D subjects.

## Acknowledgements

The authors acknowledge financial support from the Portuguese Foundation for Science and Technology (research grants PTDC/EEB-BIO/99810/2008, PTDC-SAU-MET-111398-2009, PTDC/DTP-EPI/0207/2012 and EXCL/DTP-PIC/0069/2012). The NMR spectrometers are part of the National NMR Network and were purchased in the framework of the National Programme for Scientific re-equipment, contract REDE/1517/RMN/2005, with funds from POCI 2010 (FEDER) and the Portuguese Foundation for Science and Technology. T. C. D. and F. O. M. held a fellowship from the Fundação para a Ciência e Tecnologia, Portugal (SFRH/BPD/46197/2008 and SFRH/BD/51194/2010 respectively).

## Author contributions

F. O. M., T. C. D., J. V. and J. M. G. performed the research. F. O. M., T. C. D., M. P. M. and J. G. J. designed the research study. D. K. S. and R. O. contributed essential reagents or tools. F. O. M., T. C. D., M. P. M. and J. G. J. analysed the data. F. O. M., T. C. D., M. P. M. and J. G. J. wrote the paper.

## Conflict of interest

Authors declare that they have no conflicts of interest.

## References

- Ader M, Stefanovski D, Kim SP, Richey JM, Ionut V, Catalano KJ *et al.* (2014). Hepatic insulin clearance is the primary determinant of insulin sensitivity in the normal dog. *Obesity (Silver Spring)* 22: 1238–1245.
- Afonso RA, Patarrao RS, Macedo MP, Carmo MM (2006). Carvedilol action is dependent on endogenous production of nitric oxide. *Am J Hypertens* 19: 419–425.
- Ahren B, Thorsson O (2003). Increased insulin sensitivity is associated with reduced insulin and glucagon secretion and increased insulin clearance in man. *J Clin Endocrinol Metab* 88: 1264–1270.
- Alexander SPH, Benson HE, Faccenda E, Pawson AJ, Sharman JL, Spedding M *et al.* (2013a). The Concise Guide to PHARMACOLOGY 2013/14: nuclear hormone receptors. *Br J Pharmacol.* 170: 1652–1675.
- Alexander SPH, Benson HE, Faccenda E, Pawson AJ, Sharman JL, Spedding M *et al.* (2013b). The Concise Guide to PHARMACOLOGY 2013/14: catalytic receptors. *Br J Pharmacol.* 170: 1676–1705.

- Alexander SPH, Benson HE, Faccenda E, Pawson AJ, Sharman JL, Spedding M *et al.* (2013c). The Concise Guide to PHARMACOLOGY 2013/14: enzymes. *Br J Pharmacol* 170: 1797–1867.
- Aljada A, Ghanim H, Friedman J, Garg R, Mohanty P, Dandona P (2001). Troglitazone reduces the expression of PPAR $\gamma$  while stimulating that of PPAR $\alpha$  in mononuclear cells in obese subjects. *J Clin Endocrinol Metab* 86: 3130–3133.
- Arioglu E, Duncan-Morin J, Sebring N, Rother KI, Gottlieb N, Lieberman J *et al.* (2000). Efficacy and safety of troglitazone in the treatment of lipodystrophy syndromes. *Ann Intern Med* 133: 263–274.
- Banks AS, McAllister FE, Camporez JP, Zushin PJ, Jurczak MJ, Laznik-Bogoslavski D *et al.* (2015). An ERK/Cdk5 axis controls the diabetogenic actions of PPAR $\gamma$ . *Nature* 517: 391–395.
- Bedoucha M, Atzpodiene E, Boelsterli UA (2001). Diabetic KKA $\gamma$  mice exhibit increased hepatic PPAR $\gamma$ 1 gene expression and develop hepatic steatosis upon chronic treatment with antidiabetic thiazolidinediones. *J Hepatol* 35: 17–23.
- Belfort R, Harrison SA, Brown K, Darland C, Finch J, Hardies J *et al.* (2006). A placebo-controlled trial of pioglitazone in subjects with nonalcoholic steatohepatitis. *N Engl J Med* 355: 2297–2307.
- Beysen C, Murphy EJ, Nagaraja H, Decaris M, Riiff T, Fong A *et al.* (2008). A pilot study of the effects of pioglitazone and rosiglitazone on de novo lipogenesis in type 2 diabetes. *J Lipid Res* 49: 2657–2663.
- Boden G, Homko C, Mozzoli M, Showe LC, Nichols C, Cheung P (2005). Thiazolidinediones upregulate fatty acid uptake and oxidation in adipose tissue of diabetic patients. *Diabetes* 54: 880–885.
- Bril F, Lomonaco R, Orsak B, Ortiz-Lopez C, Webb A, Tio F *et al.* (2014). Relationship between disease severity, hyperinsulinemia, and impaired insulin clearance in patients with nonalcoholic steatohepatitis. *Hepatology* 59: 2178–2187.
- Burant CF, Sreenan S, Hirano K, Tai TA, Lohmiller J, Lukens J *et al.* (1997). Troglitazone action is independent of adipose tissue. *J Clin Invest* 100: 2900–2908.
- Chong MF, Fielding BA, Frayn KN (2007). Metabolic interaction of dietary sugars and plasma lipids with a focus on mechanisms and *de novo* lipogenesis. *Proc Nutr Soc* 66: 52–59.
- Cordes CM, Bennett RG, Siford GL, Hamel FG (2009). Nitric oxide inhibits insulin-degrading enzyme activity and function through S-nitrosylation. *Biochem Pharmacol* 77: 1064–1073.
- Daly ME, Vale C, Walker M, Littlefield A, Alberti KG, Mathers JC (1998). Acute effects on insulin sensitivity and diurnal metabolic profiles of a high-sucrose compared with a high-starch diet. *Am J Clin Nutr* 67: 1186–1196.
- Delgado TC, Pinheiro D, Caldeira M, Castro MM, Gerales CF, Lopez-Larrubia P *et al.* (2009). Sources of hepatic triglyceride accumulation during high-fat feeding in the healthy rat. *NMR Biomed* 22: 310–317.
- Duckworth WC, Bennett RG, Hamel FG (1998). Insulin degradation: progress and potential. *Endocr Rev* 19: 608–624.
- Esterson YB, Zhang K, Koppaka S, Kehlenbrink S, Kishore P, Raghavan P *et al.* (2013). Insulin sensitizing and anti-inflammatory effects of thiazolidinediones are heightened in obese patients. *J Invest Med* 61: 1152–1160.
- Ferre P (2004). The biology of peroxisome proliferator-activated receptors: relationship with lipid metabolism and insulin sensitivity. *Diabetes* 53 (Suppl 1): S43–S50.
- Gastaldelli A, Miyazaki Y, Mahankali A, Berria R, Pettiti M, Buzzigoli E *et al.* (2006). The effect of pioglitazone on the liver: role of adiponectin. *Diabetes Care* 29: 2275–2281.
- Guan HP, Li Y, Jensen MV, Newgard CB, Steppan CM, Lazar MA (2002). A futile metabolic cycle activated in adipocytes by antidiabetic agents. *Nat Med* 8: 1122–1128.
- Hamel FG (2009). Preliminary report: inhibition of cellular proteasome activity by free fatty acids. *Metabolism* 58: 1047–1049.
- Hennes MM, Dua A, Kissebah AH (1997). Effects of free fatty acids and glucose on splanchnic insulin dynamics. *Diabetes* 46: 57–62.
- Huang CY, Lin YS, Chen GC, Huang HL, Chuang SH, Chao PM (2010). Upregulation of lipogenesis and protein tyrosine phosphatase-1B expression in the liver of Wistar rats with metabolic syndrome chronically induced by drinking sucrose water. *Ann Nutr Metab* 57: 169–176.
- Jones JG, Merritt M, Malloy C (2001). Quantifying tracer levels of  $^2\text{H}_2\text{O}$  enrichment from microliter amounts of plasma and urine by  $^2\text{H}$  NMR. *Magn Reson Med* 45: 156–158.
- Kawaguchi K, Sakaida I, Tsuchiya M, Omori K, Takami T, Okita K (2004). Pioglitazone prevents hepatic steatosis, fibrosis, and enzyme-altered lesions in rat liver cirrhosis induced by a choline-deficient L-amino acid-defined diet. *Biochem Biophys Res Commun* 315: 187–195.
- Khoursheed M, Miles PD, Gao KM, Lee MK, Moossa AR, Olefsky JM (1995). Metabolic effects of troglitazone on fat-induced insulin resistance in the rat. *Metabolism* 44: 1489–1494.
- Kilkenny C, Browne W, Cuthill IC, Emerson M, Altman DG (2010). NC3Rs Reporting Guidelines Working Group. *Br J Pharmacol* 160: 1577–1579.
- Kim SH, Abbasi F, Chu JW, McLaughlin TL, Lamendola C, Polonsky KS *et al.* (2005). Rosiglitazone reduces glucose-stimulated insulin secretion rate and increases insulin clearance in nondiabetic, insulin-resistant individuals. *Diabetes* 54: 2447–2452.
- Kohjima M, Higuchi N, Kato M, Kotoh K, Yoshimoto T, Fujino T *et al.* (2008). SREBP-1c, regulated by the insulin and AMPK signaling pathways, plays a role in nonalcoholic fatty liver disease. *Int J Mol Med* 21: 507–511.
- Lamontagne J, Jalbert-Arsenault E, Pepin E, Peyot ML, Ruderman NB, Nolan CJ *et al.* (2013). Pioglitazone acutely reduces energy metabolism and insulin secretion in rats. *Diabetes* 62: 2122–2129.
- Lauer B, Tuschl G, Kling M, Mueller SO (2009). Species-specific toxicity of diclofenac and troglitazone in primary human and rat hepatocytes. *Chem Biol Interact* 179: 17–24.
- Lee MK, Miles PD, Khoursheed M, Gao KM, Moossa AR, Olefsky JM (1994). Metabolic effects of troglitazone on fructose-induced insulin resistance in the rat. *Diabetes* 43: 1435–1439.
- Lehmann JM, Moore LB, Smith-Oliver TA, Wilkison WO, Willson TM, Kliewer SA (1995). An antidiabetic thiazolidinedione is a high affinity ligand for peroxisome proliferator-activated receptor gamma (PPAR gamma). *J Biol Chem* 270: 12953–12956.
- Maianti JP, McFedries A, Foda ZH, Kleiner RE, Du XQ, Leissring MA *et al.* (2014). Anti-diabetic activity of insulin-degrading enzyme inhibitors mediated by multiple hormones. *Nature* 511: 94–98.
- McGrath J, Drummond G, McLachlan E, Kilkenny C, Wainwright C (2010). Guidelines for reporting experiments involving animals: the ARRIVE guidelines. *Br J Pharmacol* 160: 1573–1576.
- Mikami T, Genma R, Nishiyama K, Ando S, Kitahara A, Natsume H *et al.* (1998). Alterations in the enzyme activity and protein contents of protein disulfide isomerase in rat tissues during fasting and refeeding. *Metabolism* 47: 1083–1088.
- Millar JS, Cromley DA, McCoy MG, Rader DJ, Billheimer JT (2005). Determining hepatic triglyceride production in mice: comparison of poloxamer 407 with Triton WR-1339. *J Lipid Res* 46: 2023–2028.

- Miners JS, Kehoe PG, Love S (2008). Immunocapture-based fluorometric assay for the measurement of insulin-degrading enzyme activity in brain tissue homogenates. *J Neurosci Methods* 169: 177–181.
- Natali A, Ribeiro R, Baldi S, Tulipani A, Rossi M, Venturi E *et al.* (2013). Systemic inhibition of nitric oxide synthesis in non-diabetic individuals produces a significant deterioration in glucose tolerance by increasing insulin clearance and inhibiting insulin secretion. *Diabetologia* 56: 1183–1191.
- Okuno A, Tamemoto H, Tobe K, Ueki K, Mori Y, Iwamoto K *et al.* (1998). Troglitazone increases the number of small adipocytes without the change of white adipose tissue mass in obese Zucker rats. *J Clin Invest* 101: 1354–1361.
- Osei K, Gaillard T, Kaplow J, Bullock M, Schuster D (2004). Effects of rosiglitazone on plasma adiponectin, insulin sensitivity, and insulin secretion in high-risk African Americans with impaired glucose tolerance test and type 2 diabetes. *Metabolism* 53: 1552–1557.
- Osei K, Gaillard T, Schuster D (2007). Thiazolidinediones increase hepatic insulin extraction in African Americans with impaired glucose tolerance and type 2 diabetes mellitus. A pilot study of rosiglitazone. *Metabolism* 56: 24–29.
- Ota T, Takamura T, Kurita S, Matsuzawa N, Kita Y, Uno M *et al.* (2007). Insulin resistance accelerates a dietary rat model of nonalcoholic steatohepatitis. *Gastroenterology* 132: 282–293.
- Pawson AJ, Sharman JL, Benson HE, Faccenda E, Alexander SP, Buneman OP *et al.* (2014). The IUPHAR/BPS Guide to PHARMACOLOGY: an expert-driven knowledgebase of drug targets and their ligands. *Nucl. Acids Res.* 42 (Database Issue): D1098–D1106.
- Pivovarova O, Gogebakan O, Pfeiffer AF, Rudovich N (2009). Glucose inhibits the insulin-induced activation of the insulin-degrading enzyme in HepG2 cells. *Diabetologia* 52: 1656–1664.
- Polonsky KS, Pugh W, Jaspan JB, Cohen DM, Karrison T, Tager HS *et al.* (1984a). C-peptide and insulin secretion. Relationship between peripheral concentrations of C-peptide and insulin and their secretion rates in the dog. *J Clin Invest* 74: 1821–1829.
- Polonsky KS, Rubenstein AH (1984). C-peptide as a measure of the secretion and hepatic extraction of insulin. Pitfalls and limitations. *Diabetes* 33: 486–494.
- Radziuk J, Morishima T (1985). New methods for the analysis of insulin kinetics *in vivo*: insulin secretion, degradation, systemic dynamics and hepatic extraction. *Adv Exp Med Biol* 189: 247–276.
- Ratzliff V, Poynard T (2006). Assessing the outcome of nonalcoholic steatohepatitis? It's time to get serious. *Hepatology* 44: 802–805.
- Richelsen B (2013). Sugar-sweetened beverages and cardio-metabolic disease risks. *Curr Opin Clin Nutr Metab Care* 16: 478–484.
- Root P, Sliskovic I, Mutus B (2004). Platelet cell-surface protein disulphide-isomerase mediated S-nitrosoglutathione consumption. *Biochem J* 382 (Pt 2): 575–580.
- Santure M, Pitre M, Nadeau A, Bachelard H (2003). Effect of troglitazone on vascular and glucose metabolic actions of insulin in high-sucrose-fed rats. *Metabolism* 52: 978–986.
- Schleicher J, Tokarski C, Marbach E, Matz-Soja M, Zellmer S, Gebhardt R *et al.* (2015). Zonation of hepatic fatty acid metabolism - The diversity of its regulation and the benefit of modeling. *Biochimica et biophysica acta* 1851: 641–656.
- Soares AF, Carvalho RA, Veiga FJ, Alves MG, Martins FO, Viegas I *et al.* (2012). Restoration of direct pathway glycogen synthesis flux in the STZ-diabetes rat model by insulin administration. *Am J Physiol Endocrinol Metab* 303: E875–E885.
- Sotiropoulos KB, Clermont A, Yasuda Y, Rask-Madsen C, Mastumoto M, Takahashi J *et al.* (2006). Adipose-specific effect of rosiglitazone on vascular permeability and protein kinase C activation: novel mechanism for PPAR $\gamma$  agonist's effects on edema and weight gain. *FASEB J* 20: 1203–1205.
- Tenenbaum A, Fisman EZ (2012). Fibrates are an essential part of modern anti-dyslipidemic arsenal: spotlight on atherogenic dyslipidemia and residual risk reduction. *Cardiovasc Diabetol* 11: 125.
- Wallace TM, Levy JC, Matthews DR (2004). Use and abuse of HOMA modeling. *Diabetes Care* 27: 1487–1495.
- Watanabe T, Furukawa T, Sharyo S, Ohashi Y, Yasuda M, Takaoka M *et al.* (2000). Effect of troglitazone on the liver of a Gunn rat model of genetic enzyme polymorphism. *J Toxicol Sci* 25: 423–431.
- Way JM, Harrington WW, Brown KK, Gottschalk WK, Sundseth SS, Mansfield TA *et al.* (2001). Comprehensive messenger ribonucleic acid profiling reveals that peroxisome proliferator-activated receptor gamma activation has coordinate effects on gene expression in multiple insulin-sensitive tissues. *Endocrinology* 142: 1269–1277.
- Wei X, Ke B, Zhao Z, Ye X, Gao Z, Ye J (2014). Regulation of insulin degrading enzyme activity by obesity-associated factors and pioglitazone in liver of diet-induced obese mice. *PLoS One* 9: e95399.
- Xiao C, Giacca A, Carpentier A, Lewis GF (2006). Differential effects of monounsaturated, polyunsaturated and saturated fat ingestion on glucose-stimulated insulin secretion, sensitivity and clearance in overweight and obese, non-diabetic humans. *Diabetologia* 49: 1371–1379.
- Yamamoto Y, Yamazaki H, Ikeda T, Watanabe T, Iwabuchi H, Nakajima M *et al.* (2002). Formation of a novel quinone epoxide metabolite of troglitazone with cytotoxicity to HepG2 cells. *Drug Metabol Dispos: Biol Fate Chemicals* 30: 155–160.
- Zai A, Rudd MA, Scribner AW, Loscalzo J (1999). Cell-surface protein disulfide isomerase catalyzes transnitrosation and regulates intracellular transfer of nitric oxide. *J Clin Invest* 103: 393–399.